Molecular Biology of the Cell
Vol. 10, 1337–1351, May 1999

Apg7p/Cvt2p Is Required for the Cytoplasm-to-Vacuole Targeting, Macroautophagy, and Peroxisome Degradation Pathways

John Kim, Valerie M. Dalton, Kimberly P. Eggerton, Sidney V. Scott, and Daniel J. Klionsky*

Section of Microbiology, University of California, Davis, California 95616

Submitted November 3, 1998; Accepted February 16, 1999
Monitoring Editor: Randy W. Schekman

Proper functioning of organelles necessitates efficient protein targeting to the appropriate subcellular locations. For example, degradation in the fungal vacuole relies on an array of targeting mechanisms for both resident hydrolases and their substrates. The particular processes that are used vary depending on the available nutrients. Under starvation conditions, macroautophagy is the primary method by which bulk cytosol is sequestered into autophagic vesicles (autophagosomes) destined for this organelle. Molecular genetic, morphological, and biochemical evidence indicates that macroautophagy shares much of the same cellular machinery as a biosynthetic pathway for the delivery of the vacuolar hydrolase, aminopeptidase I, via the cytoplasm-to-vacuole targeting (Cvt) pathway. The machinery required in both pathways includes a novel protein modification system involving the conjugation of two autophagy proteins, Apg12p and Apg5p. The conjugation reaction was demonstrated to be dependent on Apg7p, which shares homology with the E1 family of ubiquitin-activating enzymes. In this study, we demonstrate that Apg7p functions at the sequestration step in the formation of Cvt vesicles and autophagosomes. The subcellular localization of Apg7p fused to green fluorescent protein (GFP) indicates that a subpopulation of Apg7pGFP becomes membrane associated in an Apg12p-dependent manner. Subcellular fractionation experiments also indicate that a portion of the Apg7p pool is pelletable under starvation conditions. Finally, we demonstrate that the *Pichia pastoris* homologue Gsa7p that is required for peroxisome degradation is functionally similar to Apg7p, indicating that this novel conjugation system may represent a general nonclassical targeting mechanism that is conserved across species.

INTRODUCTION

The efficient turnover and recycling of proteins and redundant organelles are critical features of cell metabolism and physiology. In order to survive starvation conditions, nonessential cytosolic proteins and organelles must be delivered to the vacuole, where they are broken down and reused for essential cellular processes through the action of an array of vacuolar enzymes (reviewed by Klionsky *et al.*, 1990; Klionsky, 1997). The secretory pathway and endocytosis define the classic paradigms for the vacuolar localization of both resident hydrolases and degradative substrates, respectively. For biosynthetic delivery, most characterized vacuolar enzymes transit through the early stages of the secretory pathway. They are diverted from being secreted at the trans-Golgi network and subsequently travel directly to the vacuole or arrive at the organelle via an endosomal intermediate (reviewed by Bryant and Stevens, 1998). Similarly, proteins destined for degradation transit from the cell surface or extracellular space by endocytosis to an endosomal compartment before their ultimate delivery to the vacuole (reviewed by Riezman *et al.*, 1996). However, recent studies have demonstrated that alternate, nonclassical routes to the vacuole exist for

* Corresponding author. E-mail address: djklionsky@ucdavis.edu.

both transport of the resident hydrolase aminopeptidase I (API)[1] as well as delivery of cytoplasmic substrates (Klionsky *et al.*, 1992; and reviewed by Scott and Klionsky, 1998).

Substrates destined for degradation are delivered to the vacuole through both specific and nonspecific recycling processes. The turnover of bulk cytosol is accomplished through macroautophagy, which is induced under conditions of nutrient deprivation (Takeshige *et al.*, 1992; Baba *et al.*, 1994). Cytosolic double-membrane autophagosomes sequester proteins and organelles for subsequent transport to the vacuole (Baba *et al.*, 1994, 1995). In addition to the nonspecific process of autophagy, cells must specifically deliver targeted organelles for degradation under various nutrient conditions. For example, peroxisomes proliferate in response to certain growth conditions such as the presence of methanol or oleic acid as the sole carbon source. When glucose becomes available, peroxisomes, but not other organelles, are specifically sequestered and delivered to the vacuole for degradation by a process known as pexophagy (reviewed by Klionsky, 1997; and Scott and Klionsky, 1998). Peroxisome degradation is morphologically similar to nonspecific autophagy; however, the processes differ in the conditions for induction, the site of sequestration, and the kinetics of vacuolar delivery.

Molecular genetic analyses of both pexophagy and macroautophagy have begun to allow the isolation of mutants defective in these processes. The *pdd*, *gsa*, and *pag* mutants are blocked in various steps of peroxisome degradation (Titorenko *et al.*, 1995; Tuttle and Dunn, 1995; Sakai *et al.*, 1998). At present, however, only three of the corresponding genes have been identified (Yuan *et al.*, 1997, 1999; Kiel *et al.*, in press). Similar studies on autophagy have resulted in the identification of mutants, *apg* and *aut*, comprising ~20 complementation groups that are defective in nonspecific protein delivery to the vacuole (Tsukada and Ohsumi, 1993; Thumm *et al.*, 1994; Harding *et al.*, 1996). While substantial progress has been made in cloning the *apg* and *aut* genes and characterizing the gene products (Kametaka *et al.*, 1996; Funakoshi *et al.*, 1997; Matsuura *et al.*, 1997; Schlumpberger *et al.*, 1997; Straub *et al.*, 1997; Lang *et al.*, 1998; Mizushima *et al.*, 1998), key questions remain concerning the mechanism of sequestration and vacuolar delivery.

Simultaneous to these studies of macroautophagy, investigations into the transport of the resident vacuolar hydrolase API revealed that it is localized to the vacuole independent of the secretory pathway (Klionsky *et al.*, 1992). Biochemical and morphological studies show that API is transported to the vacuole directly from the cytoplasm via a vesicle-mediated mechanism termed the cytoplasm-to-vacuole targeting (Cvt) pathway (Baba *et al.*, 1997; Kim *et al.*, 1997; Scott *et al.*, 1997). Genetic studies resulted in the isolation of mutants, termed *cvt*, defective in API import and maturation (Harding *et al.*, 1995, 1996). Of the 15 *cvt* complementation groups, 6 overlap with previously identified autophagy mutants (Harding *et al.*, 1996; Scott *et al.*, 1996). In addition, the majority, but not all, of the remaining *cvt* mutants have autophagy defects. Similarly, the majority of nonoverlapping autophagy mutants display an API import defect (Harding *et al.*, 1996; Scott *et al.*, 1996). Taken together, these studies suggest that the Cvt pathway and autophagy utilize many of the same molecular components.

Recent studies support the overlap between the Cvt and autophagy pathways by demonstrating that API is transported to the vacuole through two overlapping processes. During vegetative growth, API utilizes the Cvt pathway, while under starvation conditions the macroautophagy pathway transports API, as well as bulk cytosol, to the vacuole (Baba *et al.*, 1997). However, in contrast to the slow, nonselective turnover of bulk cytosol, the kinetics of API import under both vegetative and starvation conditions remain relatively rapid (half-time of 30–45 min), suggesting that API maintains a specific mechanism for its delivery (Klionsky *et al.*, 1992; Scott *et al.*, 1996). The fact that API transport occurs under both vegetative and starvation conditions makes it a useful marker for the study of both the Cvt and macroautophagy pathways.

The study of API transport has begun to delineate discrete, sequential steps in the import process (Figure 1). API is synthesized in the cytosol as a 61-kDa precursor (prAPI) that includes an N-terminal 45-amino acid propeptide that is necessary for its vacuolar delivery (Oda *et al.*, 1996). After synthesis, the 61-kDa prAPI rapidly oligomerizes in the cytosol into a dodecamer with a molecular mass of 732 kDa (Figure 1, step 1; Kim *et al.*, 1997). Evidence from biochemical and electron microscopy studies indicates that prAPI subsequently forms a large protein complex in the cytosol defined as the Cvt complex (Figure 1, step 2; Baba *et al.*, 1997; Scott *et al.*, 1997). Subsequent to formation of the Cvt complex, a membrane recognition and sequestration event occurs in which the complex becomes enwrapped by a double membrane of unknown origin (Figure 1, step 3; Baba *et al.*, 1997). In this step, prAPI in the Cvt complex remains accessible to the cytosol because of the incomplete formation of the surrounding vesicle. The completion of the sequestration event results in the formation of the double-membrane Cvt vesicle under vegetative growth con-

[1] Abbreviations used: API, aminopeptidase I; Con A, concanavalin A; CPY, carboxypeptidase Y; Cvt, cytoplasm-to-vacuole targeting; GFP, green fluorescent protein; PIPES, piperazine-*N*,*N*′-bis(2-ethanesulfonic acid); SMD, synthetic minimal medium containing 2% glucose, essential amino acids, and ammonium sulfate; SD-N, synthetic minimal medium containing 2% glucose but lacking essential amino acids and ammonium sulfate; TCA, trichloroacetic acid.

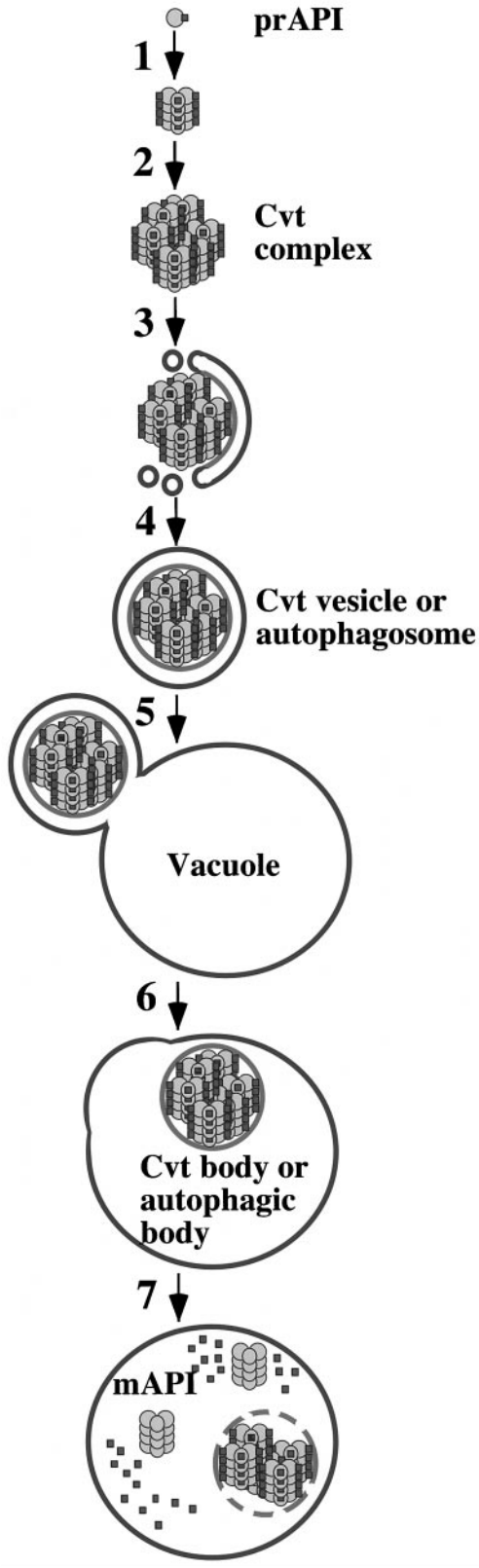

ditions and the autophagosome in starvation conditions (Figure 1, step 4; Baba *et al.*, 1997). The Cvt vesicles are ~150 nm in diameter and contain an electron-dense core that appears distinct from cytosol. Autophagosomes are ~300–900 nm in diameter and also contain the electron-dense Cvt complex, in addition to bulk cytosol (Baba *et al.*, 1994, 1995, 1997; Scott *et al.*, 1997).

Upon completion of formation, the Cvt vesicle/autophagosome is specifically targeted to the vacuole, where the outer membrane of the vesicle docks and fuses with the vacuolar membrane (Figure 1, step 5; Baba *et al.*, 1995, 1997). This fusion reaction is followed by the release of the inner membrane of the vesicle, the Cvt body, or the autophagic body into the vacuolar lumen (Figure 1, step 6; Baba *et al.*, 1994, 1995, 1997; Scott *et al.*, 1997). In the final step of the Cvt and autophagy pathways, the vesicle membrane is degraded in a vacuolar protease-dependent manner. Vesicle breakdown also requires the proper vacuolar pH (Nakamura *et al.*, 1997). The breakdown of the inner membrane vesicle allows the content of the Cvt body and the bulk cytosol inside the autophagic body to be accessible to vacuolar proteases, resulting in the processing of prAPI to its mature form as well as the degradation and recycling of bulk cytosol transported inside the autophagic bodies (Figure 1, step 7; Takeshige *et al.*, 1992; Scott *et al.*, 1997).

The *apg7/cvt2* mutants were isolated in two independent screens based on defects in autophagy and API import, respectively (Tsukada and Ohsumi, 1993; Harding *et al.*, 1995). A mutation in a homologous gene, *GSA7*, was also identified in a screen for defects in peroxisomal degradation (Yuan *et al.*, 1999). A recent study indicated that Apg7p contains considerable homology to E1 ubiquitin-activating enzymes and was required in a novel conjugation reaction of two other autophagy proteins, Apg5p and Apg12p (Mizushima *et al.*, 1998). These reactions were discovered to be essential for autophagy as well as API import via the Cvt pathway. Therefore, unlike the analogous ubiquitin-mediated, proteasome-dependent proteolysis system, the Apg7p-dependent covalent modification system is not restricted to a degradation function, but may function as part of a novel, general targeting mechanism. In this study, we sought to determine the site of function of Apg7p in the Cvt/autophagy pathways.

Figure 1. Steps in API import via the Cvt and autophagy pathways. Details are discussed in INTRODUCTION. Step 1: prAPI dodecamerization; step 2: Cvt complex formation; step 3: recognition and membrane sequestration; step 4: membrane expansion and vesicle completion; step 5: targeting, docking, and fusion of the Cvt vesicle or autophagosome with the vacuole; step 6: release of the Cvt body or autophagic body into the vacuole lumen; step 7: breakdown of the Cvt body or autophagic body and maturation of API.

We demonstrate that Apg7p is required for completion of the sequestration event and show that its interaction with membranes is dependent on its substrate Apg12p. Complementation of the *apg7* defect by the *GSA7* gene suggests that this protein functions in three overlapping but discrete pathways, autophagy, Cvt, and pexophagy.

MATERIALS AND METHODS

Strains and Media

Wild-type haploid *Saccharomyces cerevisiae* yeast strains used in this study were: SEY6210 (MATα *leu2–3112 ura3–52 his3-Δ200 trp1-Δ901 lys2–801 suc2-Δ9 GAL*) and SEY6211 (*MATa leu2–3112 ura3–52 his3-Δ200 trp1-Δ901 ade2–101 suc2-Δ9 GAL*) (Robinson *et al.*, 1988). Mutant strains THY193a (*cvt2–1*) and THY226a (*cvt2–2*), YNM101 (MATα *trp1 leu2 his3 ura3 apg12Δ::HIS3*), and WSY99 (MATα *leu2–3112 ura3–52 his3-Δ200 trp1-Δ901 lys2–801 suc2-Δ9 GAL ypt7Δ::HIS3*) were isolated and characterized previously (Harding *et al.*, 1995; Mizushima *et al.*, 1998; Wurmser and Emr, 1998, respectively).

The *apg7Δ* disruption strain VDY101 (MATα *leu2–3112 ura3–52 his3-Δ200 trp1-Δ901 lys2–801 suc2-Δ9 GAL apg7Δ::LEU2*) was generated by one-step disruption of strain SEY6210 in this study. The *apg5Δ* strain, MGY101 (MATα *leu2–3112 ura3–52 his3-Δ200 trp1-Δ901 lys2–801 suc2-Δ9 GAL apg5Δ::LEU2*) was provided by Michael George (George and Klionsky, manuscript in preparation).

Yeast strains were grown in synthetic minimal medium (SMD; 0.067% yeast nitrogen base, 2% glucose, and auxotrophic amino acids and vitamins as needed) for immunoblotting, radiolabeling, and immunoprecipitation. YPD (containing 1% yeast extract, 2% peptone, and 2% glucose) was used for cell growth before transformation. Synthetic minimal medium containing 2% glucose without ammonium sulfate or amino acids was used for nitrogen starvation experiments (SD-N).

Materials

To prepare antiserum to Apg7p, synthetic peptides corresponding to amino acids 427–443 and 606–630 of Apg7p were synthesized and conjugated individually to keyhole limpet hemocyanin (Multiple Peptide Systems; San Diego, CA). Standard procedures were used to generate antiserum in a New Zealand white rabbit. Antisera against CPY and API were prepared as described previously (Klionsky *et al.*, 1992, 1988, respectively). Antiserum against phosphoglycerate kinase was provided by Dr. Jeremy Thorner (Baum *et al.*, 1978).

All restriction enzymes and Vent DNA polymerase were from New England Biolabs (Beverly, MA). Expre^{35}S^{35}S Protein Labeling Mix was from Dupont-NEN Research Products (Boston, MA). Immobilon-P (polyvinylidene fluoride) was from Millipore (Bedford, MA). Con A Sepharose was from Pharmacia (Piscataway, NJ). Complete EDTA-free protease inhibitor cocktail was from Boehringer Mannheim Biochemicals (Indianapolis, IN). Oxalyticase was from Enzogenetics (Corvallis, OR). The Vistra ECF Western Blotting System was obtained from Amersham (Arlington Heights, IL). YNB was from Difco (Detroit, MI). YNB-copper was from BIO 101 (Vista, CA). Oligonucleotides to pBR322 were from Promega (Madison, WI); all other oligonucleotides were synthesized by Operon Technologies (Alameda, CA). Vectors for expressing GFP fusions were a gift from Dr. Jodi Nunnari (University of California, Davis). The copper-inducible promoter-based vectors, pCu416 and pCu426, were gifts from Dr. Dennis J. Thiele (Labbe and Thiele, in press). The *Pichia pastoris* plasmid pYM8 containing the *GSA7* open reading frame (ORF) was a gift from Dr. William A. Dunn, Jr. (University of Florida College of Medicine, Gainesville). All other reagents were from Sigma (St. Louis, MO).

Cloning APG7 by Nitrogen Starvation

The *cvt2/apg7* strain (Harding *et al.*, 1995) was transformed with a yeast genomic plasmid library (Rose *et al.*, 1987), and the transformants were selected on SMD-ura plates. The transformants were then pooled, resuspended in SMD-ura at a concentration of 0.5 OD_{600}/ml, and allowed to double before being transferred to SD-N media for 17 d. Survivors were plated onto SMD-ura plates and then screened by Western blot for the complementation of API maturation defect as described previously (Harding *et al.*, 1995). The complementing plasmid was recovered and sequencing (University of California, Davis, Division of Biological Sciences Automated DNA Sequencing Facility) was performed using pBR322 oligonucleotides. Partial sequences were entered in the *Saccharomyces* Genome Database (SGD; http://genome-www.stanford.edu/Saccharomyces/), which identified a region of DNA on chromosome VIII. Subsequent subclonings identified a 4.3-kilobase (kb) *Sac*II/*Kpn*I fragment that complemented the API maturation defect. This fragment contained one continuous ORF, YHR171W, corresponding to the recently identified gene *APG7* (Mizushima *et al.*, 1998). The pRS414 plasmid containing the *APG7* sequence was named pAPG7(414). The multicopy plasmid used to overexpress Apg7p, pAPG7(424), was constructed by subcloning a 3.1-kb *Sac*I/*Bam*HI fragment from pAPG7(414) into the *Sac*I/*Bam*HI sites of pRS424. The *Sac*I/*Bam*HI *APG7*-containing fragment was also subcloned into pRS416 (pAPG7(416)) and pRS426 (pAPG7(426)). All of the *APG7* plasmids complemented the API import defect by immunoblot analysis.

Disruption of the APG7 Chromosomal Locus

To disrupt the *APG7* chromosomal locus, pAPG7(414) was digested with *Xho*I/*Spe*I to remove a 694-base pair (bp) fragment from the *APG7* gene. A *Xho*I/*Xba*I fragment containing the *LEU2* gene was isolated from the plasmid pJLS2 and ligated with the *Xho*I/*Spe*I-digested pAPG7(414) to generate pAPG7Δ::LEU2. Primers to the flanking sequences of the *APG7* gene (5′-CACCCGCGGAATCTCAGCAG-3′, 5′-CGAACTTAAAACGTATTGATTGAGGGCCCG-3′) were synthesized, and the linear knockout construct was amplified by PCR. The PCR product was used to transform the yeast strain SEY6210. Transformants were selected on SMD-leu plates, and the *apg7Δ* knockout strain was identified by the accumulation of prAPI. Tetrad analysis was performed to confirm that the deleted *APG7* gene maps to the same locus as the original *cvt2/apg7* mutant: the *apg7Δ* strain was transformed with the pAPG7(416) plasmid and crossed to both alleles of *cvt2/apg7* (THY193a *cvt2–1* and THY226a *cvt2–2*). Diploids were sporulated, and the resulting 31 tetrads were dissected. Isolated tetrads were plated onto 5-Fluoro-orotic acid plates to cure the germinants of the pAPG7(416) plasmid. Colonies were then screened for the API maturation defect. All cured germinants showed a precursor API phenotype indicating that the *APG7* gene maps to the correct locus.

Construction of Apg7 Fusions with GFP

To construct the pAPG7GFP centromeric and multicopy plasmids, a cassette containing the GFP ORF and actin termination sequences was first removed from pRS305Mip1-GFP using a *Bam*HI/*Hin*dIII digest and subcloned into pRS416 and pRS426, resulting in pCGFP(416) and pCGFP(426). The *Bam*HI site was in frame with the GFP ORF. The *APG7* gene, including the 363-bp upstream sequence, was then PCR amplified from the pAPG7(414) template using oligonucleotides that incorporated a *Not*I site on the 5′-primer and an in-frame *Bam*HI site on the 3′-primer (5′-GGAGTCGAGAACGCGGCCGCTGAATCTCAG-3′, 5′-GCAATCTCATCGGATCCATCATCTTCCC-3′). The PCR product was subcloned into pCGFP(416) and pCGFP(426), resulting in pAPG7GFP(416) and pAPG7GFP(426). To test for function, the fusion plasmids were transformed into the *apg7Δ* strain and examined for the rescue of the API import defect.

Construction of APG7 and GSA7 under the CUP1 Copper-inducible Promoter

The *APG7* ORF was PCR amplified from pAPG7(414) using oligonucleotides that incorporated a *Bam*HI site on the 5′-primer and a *Sal*I site on the 3′-primer (5′-GAGGATCCAGAATAAAATGTCGTCAG-3′,5′-GTGAGTAAAGTCAAGAATTTGTCGACTTG-3′). The PCR product was digested with *Bam*HI/*Sal*I and subcloned into the *Bam*HI/*Sal*I sites in pCu416 and pCu426 (centromeric and multicopy-pRS–based vectors containing the *CUP1* copper-inducible promoter; Labbe and Thiele, in press), resulting in pCu416APG7 and pCu426APG7, respectively.

The *GSA7* ORF was PCR amplified from *P. pastoris* plasmid pYM8 containing the *GSA7* ORF (Yuan *et al.*, 1999). The oligonucleotides used in the PCR contained an engineered upstream *Bam*HI site on the 5′-primer and a downstream *Sal*I site on the 3′-primer (5′-GTCTAACCTTTAGAAGGATCCTTCCCCCAC-3′, 5′-GAGAGAAGGAGAGCAGTCGACCACTAATAAAGAG-3′). The PCR product was digested with *Bam*HI/*Sal*I and subcloned into the *Bam*HI/*Sal*I sites in pCu416 and pCu426, resulting in pCu416GSA7 and pCu426GSA7.

Cell Viability under Nitrogen Starvation Conditions

To examine the survival of various yeast strains under nitrogen starvation conditions, cells were grown to an OD_{600} = 1 in SMD, washed in SD-N, and then resuspended in SD-N to an OD_{600} = 1. For the analysis of the *apg7*Δ strain transformed with the *APG7* and *GSA7* genes under the regulable control of the *CUP1* copper-inducible promoter, cells were grown in SMD containing 100 μM $CuSO_4$ to an OD_{600} = 1 before shift into SD-N medium. At the indicated times, aliquots were removed and plated onto YPD plates in triplicate. Colonies that survived the nitrogen starvation regimen were counted after 2–3 d.

Cell Labeling and Subcellular Fractionations

For cell-labeling experiments, cells were grown to an OD_{600} = 1 and resuspended in SMD at 20–30 OD_{600}/ml. The resuspended cells were labeled with 10–20 μCi of ^{35}S Express label/OD_{600} for the indicated times followed by a chase reaction in SMD supplemented with 0.2% yeast extract, 4 mM methionine, and 2 mM cysteine at a final cell density of 1 OD_{600}/ml. The labeled cells were precipitated with 10% trichloroacetic acid (TCA) on ice, followed by two acetone washes. Crude extracts were prepared by glass-bead lysis, as described previously (Harding *et al.*, 1995).

To biochemically examine the subcellular distribution of Apg7p under vegetative growth and nitrogen starvation conditions, appropriate yeast strains were transformed with the multicopy plasmid of *APG7* [pAPG7(426)] and grown to OD_{600} = 1 in SMD or subsequently transferred into SD-N medium for 15 h. The cells were then converted into spheroplasts and subjected to subcellular fractionation procedures. Spheroplasts were prepared using a modification of a previously described protocol (Kim *et al.*, 1997). In brief, cells were incubated for 15 min at 30°C in a buffer of 0.1 M Tris-SO_4, pH 9.4, and 10–20 mM DTT. After a 5000 × *g* spin for 5 min, the cells were resuspended in an osmotically supportive spheroplasting medium (1 M sorbitol, 50 mM sodium phosphate, pH 7.4, in SMD or SD-N, depending on the growth media used) containing 1–5 μg/OD_{600} of oxalyticase and incubated for 30 min at 30°C. The spheroplasts were then pelleted at 1500 × *g* for 5 min and lysed by pipeting in a physiological salts buffer (100 mM KOAc, 50 mM KCl, 5 mM $MgCl_2$, 20 mM piperazine-*N*,*N*′-bis(2-ethanesulfonic acid) (PIPES), pH 6.8) containing a cocktail of protease inhibitors at a spheroplast density of 20 OD_{600}/ml in lysis buffer. Unlysed spheroplasts were removed by a centrifugation step at 500 × *g* for 5 min at 4°C. The precleared total lysate (T) was subjected to centrifugation at 13,000 × *g* for 10 min at 4°C and separated into supernatant and pellet fractions (S13 and P13, respectively). The S13 fraction was then subjected to centrifugation at 100,000 × *g* for 30 min at 4°C and separated into high-speed supernatant and pellet fractions (S100 and P100, respectively). Aliquots of the T, S13, P13, S100, and P100 fractions were TCA precipitated, washed in acetone, and subjected to SDS-PAGE and immunoblotting analysis.

The immunoblot procedure has been described previously (Oda *et al.*, 1996). For quantitation analysis, the immunoblotting procedure was modified, and immunodetection was executed using a Vistra ECF chemifluorescent substrate as described previously (Kim *et al.*, 1997). The procedures to test for the presence of carbohydrate using tunicamycin treatment and Con A Sepharose precipitations were followed exactly as previously described (Klionsky *et al.*, 1992). All samples from radiolabeling and quantitative immunoblot experiments were examined using the Molecular Dynamics Storm System equipped with both phosphorscreen and blue fluorescence/chemifluorescence scanners (Molecular Dynamics, Sunnyvale, CA).

Membrane Flotation Analysis

The procedure for the membrane flotation experiments is a modification of a previously described protocol (Babst *et al.*, 1997). Spheroplasts from the *apg7*Δ strain were lysed in an osmotic lysis buffer (20 mM PIPES, pH 6.8, 200 mM sorbitol, 5 mM $MgCl_2$, Complete EDTA-free protease inhibitor cocktail) on ice at a spheroplast density of 20 OD_{600}/ml. The lysate from 16 OD_{600} cell equivalents was subjected to a 5000 × *g* centrifugation for 5 min at 4°C, resulting in low-speed supernatant (S5) and pellet (P5) fractions. The P5 fractions, which contain all of the precursor API, were resuspended in 300 μl of 60% sucrose (wt/vol) in gradient buffer (GB; 20 mM PIPES, pH 6.8, 5 mM $MgCl_2$, Complete EDTA-free protease inhibitor cocktail) with or without the addition of 1% Triton X-100. The resuspended P5 fractions were overlaid with 900 μl of 55% sucrose in GB and then 900 μl of 35% sucrose in GB. The resulting step gradients were subjected to centrifugation at 100,000 × *g* for 60 min at 4°C. Fractions were collected from the top. The first 1.2 ml was the float fraction, the remaining 900 μl was the nonfloat fraction, and the gradient pellet was considered the pellet fraction. The resulting fractions were TCA precipitated and washed twice with acetone before being subjected to immunoblot analysis with anti-API antiserum.

Protease Sensitivity Analysis

To examine the protease sensitivity of API in the *apg7*Δ and *ypt7*Δ strains, spheroplasts were lysed in the osmotic lysis buffer at a spheroplast density of 20 OD_{600}/ml. The resulting lysate (20 OD_{600} cell equivalents per incubation condition) was separated into S5 supernatant and P5 pellet fractions by centrifugation at 5000 × *g* for 5 min at 4°C. The P5 pellet was resuspended in osmotic lysis buffer in the presence or absence of proteinase K (50 μg/ml) and 0.2% Triton X-100. The resuspended P5 pellets were incubated on ice for 30 min, followed by TCA precipitation, acetone wash, and immunoblot analysis with anti-API antiserum.

Fluorescence Microscopy

Strains with Apg7pGFP fusion protein were grown to midlog stage in SMD medium and shifted to SD-N for 8–20 h. Cells were examined on a Leica DM IRB confocal microscope (Leica, Deerfield, IL) utilizing a 410- to 425-nm band pass filter. The images captured were the result of an average of eight scans of a single focal plane. For analysis of fluorescent cell populations (Table 1), a Nikon Axiophot epifluorescence microscope (Nikon, Garden City, NY) was used.

Copper-induced Expression Analysis

To examine the expression of Apg7p and Gsa7p under the regulable control of the *CUP1* copper-inducible promoter, the appropriate strains were grown to 0.2 OD_{600}/ml in SMD lacking copper and then induced with 100 mM $CuSO_4$ for 7 h. In the 0 μM $CuSO_4$

Table 1. Apg7pGFP displays an Apg12p-dependent punctate staining pattern upon shift to nitrogen starvation conditions

Time in SD-N (h)	Strain	Total cells counted	Fluorescent cells detected	% Fluorescent cells[a]	Cells with punctate staining	% Cells with punctate staining[b]
0	Wild-type	291; 406	130; 160	42 ± 4	0; 0	0 ± 0
4	Wild-type	368; 451	136; 203	41 ± 6	30; 49	23 ± 1
15	Wild-type	633; 597	293; 225	42 ± 6	122; 78	38 ± 5
0	*apg5*Δ	211; 436	138; 272	64 ± 2	0; 0	0 ± 0
4	*apg5*Δ	233; 327	139; 184	58 ± 2	33; 41	23 ± 1
15	*apg5*Δ	465; 670	311; 421	65 ± 3	220; 310	72 ± 2
0	*apg12*Δ	293; 603	154; 362	56 ± 5	0; 0	0 ± 0
4	*apg12*Δ	183; 247	120; 127	58 ± 10	3; 0	1 ± 2
15	*apg12*Δ	548; 479	337; 297	62 ± 1	0; 0	0 ± 0

[a] The percent of total cells counted that were fluorescent.

[b] The percent of fluorescent cells that exhibited punctate structures.

cultures, bathocuproinedisulfonic acid copper chelator was added to a final concentration of 100 μM. Cells were then harvested and examined by immunoblot analysis.

RESULTS

Apg7p Is a Component of Both the Macroautophagy and Cvt Pathways

Genetic mutants in the Cvt pathway were originally isolated on the basis of their precursor API accumulation phenotype. Further analysis revealed that the majority of these *cvt* mutants share a genetic overlap with mutants defective in macroautophagy (Harding *et al.*, 1996; Scott *et al.*, 1996). For example, *cvt2* was found to be allelic to *apg7* and demonstrated both sensitivity to nitrogen starvation conditions as well as a defect in API transport. Therefore, survival in nitrogen-poor medium offered a convenient initial selection strategy to clone the complementing gene for the *cvt2/apg7* mutant. The sequence of the *APG7* gene was recently published (Mizushima *et al.*, 1998). Accordingly, we will use the *APG7* nomenclature hereafter in this study.

The *apg7* mutant was transformed with a yeast genomic library (Rose *et al.*, 1987), grown to early-log phase, and transferred to synthetic minimal medium lacking nitrogen (SD-N) for 17 d. As a secondary screen, transformants that survived the nitrogen starvation regimen were examined by immunoblot analysis for complementation of the precursor API mutant phenotype. The genomic library plasmids from transformants that passed both screenings were isolated. Partial sequences from these complementing genomic plasmids were entered into the *Saccharomyces* Genome Database (SGD) to obtain full-length sequences, which contained overlapping fragments of 7–8 kb. Subcloning allowed the identification of an ORF that rescued the API-processing defect in the *apg7* mutant. A strain in which 37% of the *apg7*-complementing ORF was deleted and replaced by the *LEU2* auxotrophic marker showed the precursor API accumulation phenotype (Figure 2A, lane 3), confirming that Apg7p is required for API import. Subsequent tetrad analysis revealed that the deleted gene mapped to the same locus as the original *apg7* mutant gene (our unpublished results). The API-processing defect in *apg7*Δ was rescued by the *APG7* gene on centromeric or multicopy plasmids (Figure 2A). In addition, survival in nitrogen starvation was also restored in the *apg7*Δ strain transformed with the *APG7* centromeric plasmid (Figure 2B), suggesting that Apg7p is a shared component of both macroautophagy and API import by the Cvt pathway.

Precursor API Is Membrane Associated in the apg7Δ Strain

Once synthesized in the cytoplasm, precursor API rapidly forms a dodecamer and assembles into a pelletable Cvt complex (Baba *et al.*, 1997; Kim *et al.*, 1997). Biochemical and electron microscopy studies have demonstrated that the Cvt complex is subsequently enwrapped by a membrane to form the Cvt vesicle (Baba *et al.*, 1997; Scott *et al.*, 1997). Membrane flotation experiments were performed to assess the stage of API import in which accumulated prAPI is blocked in the *apg7*Δ strain. In this analysis, membrane-associated proteins would be recovered in the float (F) fraction, while soluble proteins would remain in the nonfloat (NF) fraction, and proteins associated with large, protein complexes would be recovered as a gradient pellet (P2).

Spheroplasts were prepared from the *apg7*Δ strain and subjected to differential osmotic lysis, which preserves the membrane integrity of the vacuole while disrupting the plasma membrane. After a 5000 × *g* low-speed centrifugation step, prAPI was

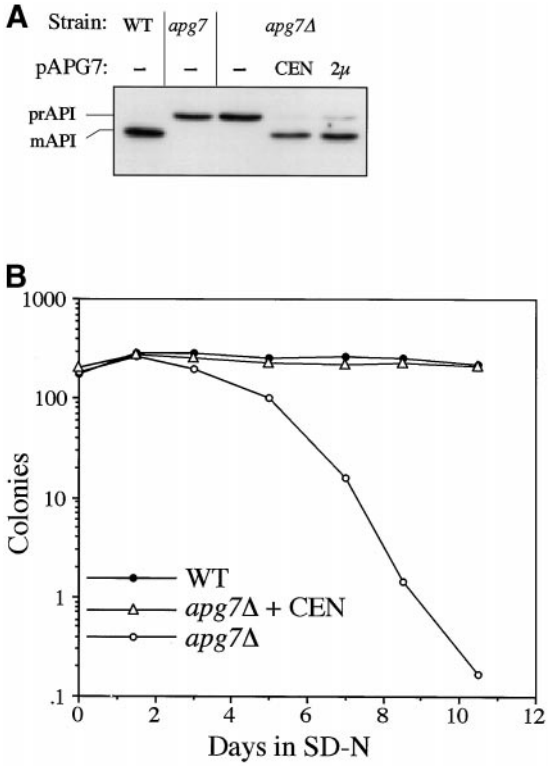

Figure 2. Cloning and characterization of *APG7*. (A) WT (wild-type, SEY6210), *apg7* (THY193), *apg7*Δ (VDY1), and the *apg7*Δ strain transformed with single copy (CEN, pAPG7(414)) or multicopy (2 μ, pAPG7(424)) plasmids encoding *APG7* were grown to log phase in SMD. Protein extracts were prepared and analyzed by immunoblot using antiserum to API as described in MATERIALS AND METHODS. The positions of precursor and mature API are indicated. The *APG7* gene complements the precursor API accumulation phenotype of the *apg7*Δ mutant. (B) WT (wild-type, SEY6210), *apg7*Δ (VDY1), and the *apg7*Δ strain transformed with the *APG7* centromeric plasmid pAPG7(414) were grown in SMD and transferred to SD-N as described in MATERIALS AND METHODS. Aliquots were removed at the indicated times and spread onto YPD plates in triplicate. Numbers of viable colonies were determined after 2–3 d. The *APG7* gene complements the starvation-sensitive phenotype of the *apg7*Δ mutant.

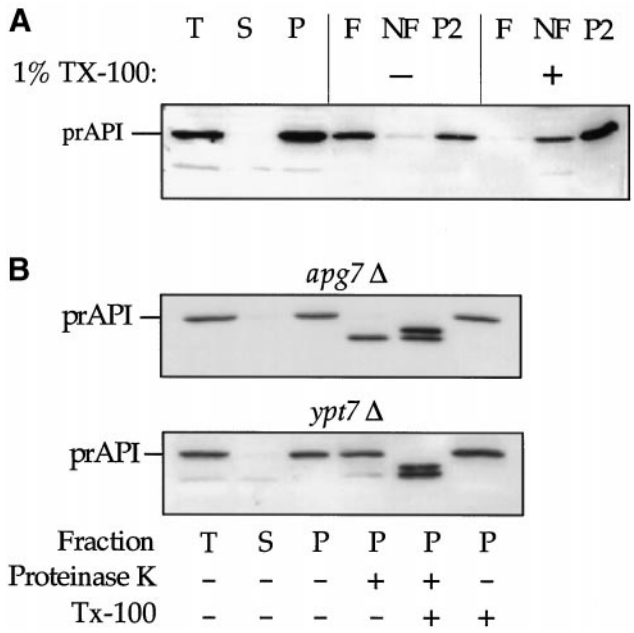

Figure 3. The *apg7*Δ mutant accumulates precursor API in a membrane-associated and protease-sensitive form that is part of a large complex. (A) The *apg7*Δ strain (VDY1) was grown in SMD to midlog phase and converted to spheroplasts. The spheroplasts were lysed in osmotic lysis buffer (see MATERIALS AND METHODS). An aliquot was removed for a total lysate control (T). The remainder of the lysed spheroplasts were separated into supernatant (S) and pellet (P) fractions by centrifugation at 5000 × *g*. The pellet fraction was resuspended in 60% sucrose in GB in the presence or absence of Triton X-100 and overlaid with 55 and 35% sucrose in GB. The step gradients were centrifuged at 100,000 × *g* for 60 min. Membrane-containing float (F), nonfloat (NF), and pellet (P2) fractions were collected and subjected to immunoblot analysis with antiserum to API as described in MATERIALS AND METHODS. The position of precursor API is indicated. (B) Precursor API in *apg7*Δ is protease accessible. Spheroplasts isolated from *apg7*Δ (VDY1) and *ypt7*Δ (WSY99) cells were lysed in osmotic lysis buffer. Supernatant (S) and pellet (P) fractions after a 5000 × *g* centrifugation were collected, and the pellet fractions were subjected to protease treatment in the absence or presence of 0.2% Triton X-100 as described in MATERIALS AND METHODS. The resulting samples were subjected to immunoblot analysis with antibody against API.

recovered entirely in a pelletable (P) fraction (Figure 3A). This pellet fraction was then subjected to the membrane flotation step gradient. In the *apg7*Δ strain, the majority of prAPI was found in the float fraction (F) in the absence of detergent, suggesting that it is directly or indirectly membrane-associated (Figure 3). In addition, a large fraction was also found in the P2 pellet fraction, indicating that a significant portion of prAPI is part of a large pelletable complex (Figure 3A). In the presence of detergent, the majority of prAPI was recovered from the P2 pellet with only a minor amount recovered in the soluble protein pool of the nonfloat fraction. These findings suggest that prAPI in *apg7*Δ is part of a large protein complex that, in part, associates with a membraneous compartment. In addition, prAPI maintains its binding to the protein complex even after the membrane association has been disrupted by detergent treatment.

Apg7p Acts at the Step of Vesicle Formation

In the *apg7*Δ strain, the precursor form of API accumulates in a large pelletable complex that associates with a membrane. We next wanted to examine whether the accumulated prAPI was accessible to protease treatment. If Apg7p is required for the comple-

tion of vesicle formation (Figure 1, step 4), then prAPI would be sensitive to exogenously added proteases and processed to the mature form in the *apg7*Δ strain. Alternatively, if Apg7p functions at a downstream event after the completion of the enwrapping membrane, then prAPI would remain in a protease-protected precursor state. This protease-protected phenotype is observed in mutants blocked in fusion of vesicles with the vacuole, such as *vps18 ts* (Scott *et al.*, 1997), *vam3 ts* (Darsow *et al.*, 1997) and *ypt7*Δ. Ypt7p is a rab guanosine triphosphatase required for homotypic vacuole fusion (Haas *et al.*, 1995). In addition, the *ypt7*Δ strain displays a strong block in the maturation of API in both rich and starvation conditions, suggesting that it is required for both the delivery of Cvt and macroautophagic vesicles to the vacuole (our unpublished results).

To investigate whether Apg7p functions in the vesicle formation step of API targeting, a protease-protection assay was performed. Protease-accessible precursor API is usually digested to the mature form by exogenous protease. This presumably reflects the protease-resistant nature of mature API as a resident vacuolar hydrolase. Spheroplasts from both the *apg7*Δ and *ypt7*Δ strains were lysed osmotically and separated into low-speed supernatant and pellet fractions. In both strains, prAPI was recovered in the membrane-associated pellet fraction (Figure 3B). When the pellet fraction was subjected to proteinase K digestion in the *apg7*Δ strain, prAPI was completely sensitive to proteolysis (Figure 3B), independent of detergent addition, suggesting that the surrounding membrane had not completely formed. However, prAPI in the *ypt7*Δ strain was protected from exogenously added proteinase K and was only protease accessible after the addition of detergent (Figure 3B). In both strains, detergent treatment in the absence of protease did not alter the prAPI pattern (Figure 3B). These findings suggest that Apg7p is required for the complete formation of the vesicle around the prAPI protein complex (Figure 1, step 4), while Ypt7p acts at a downstream event after vesicle formation has been completed (Figure 1, step 5).

Apg7p Biosynthesis

A previous study revealed that Apg7p shows significant homology with E1 ubiquitin-activating enzymes in *S. cerevisiae* as well as in other species (Mizushima *et al.*, 1998; Tanida *et al.*, 1999). The deduced amino acid sequence of Apg7p predicts a 630-amino acid protein with a molecular mass of 71.4 kDa. To further characterize Apg7p, antiserum to the protein was raised against two synthetic peptides. To examine the expression of Apg7p, wild-type and *apg7*Δ strains harboring the centromeric or multicopy *APG7* plasmid were radiolabeled for 10 min. After cell lysis, the extracts were subjected to immunoprecipitation with the anti-Apg7p antibody (Figure 4A). Immunoprecipitated Apg7p migrates at the predicted size of 71 kDa by SDS-PAGE. The 71-kDa band is absent in the *apg7*Δ strain (Figure 4A) and shows a dose-dependent increase in level in strains bearing plasmids that encode the *APG7* gene (Figure 4A). These data suggest that the 71-kDa band corresponds to Apg7p.

To determine whether Apg7p undergoes proteolytic processing, a detailed pulse/chase analysis was performed (Figure 4B). Wild-type cells were radiolabeled for 10 min, followed by a nonradioactive chase. Immunoprecipitation analysis under reducing conditions indicated that Apg7p does not undergo any apparent proteolytic processing after synthesis (Figure 4B, bottom panel). As a control, we examined API, which was shown to be processed from the 61-kDa precursor form to the 50-kDa mature enzyme with a half-time of 30 min (Figure 4B, top panel).

Sequence analysis of Apg7p revealed several potential sites for the addition of N-linked oligosaccharides. Addition of carbohydrate moieties would result in an increase in molecular mass that should be detectable by SDS-PAGE. However, Apg7p did not show a glycosylation-dependent modification over a 3-h time course based on this criterion (Figure 4B). To confirm that Apg7p is not glycosylated, we tested for the presence of N-linked and O-linked oligosaccharides through the use of tunicamycin and Con A (concanavalin A) (Figure 4C). Tunicamycin-treated N-linked glycoproteins migrate as a lower-molecular-mass species by SDS-PAGE while Con A lectin binds to both N- and O-linked mannose-containing oligosaccharides.

Wild-type cells were incubated for 15 min in the presence or absence of tunicamycin before radiolabeling for 20 min. Half of the labeled samples were directly immunoprecipitated (total) with anti-Apg7p and carboxypeptidase Y (CPY) antibodies while the remaining sample was treated with Con A Sepharose and separated into Con A-precipitable (pellet, P) and nonprecipitable (supernatant, S) fractions before immunoprecipitation reactions. The wild-type vacuolar hydrolase CPY binds Con A in the absence of tunicamycin, consistent with its being glycosylated. However, in the presence of tunicamycin, CPY is not glycosylated and migrates as a lower molecular mass species that does not bind Con A and appears in the Con A supernatant fraction (Figure 4C, top panel). In contrast, the molecular mass of Apg7p remains unchanged in the presence or absence of tunicamycin. Similarly, under both conditions, Apg7p fails to bind Con A and remains in the Con A supernatant fraction (Figure 4C, bottom panel). These results suggest that Apg7p does not contain N- or O-linked oligosaccharides.

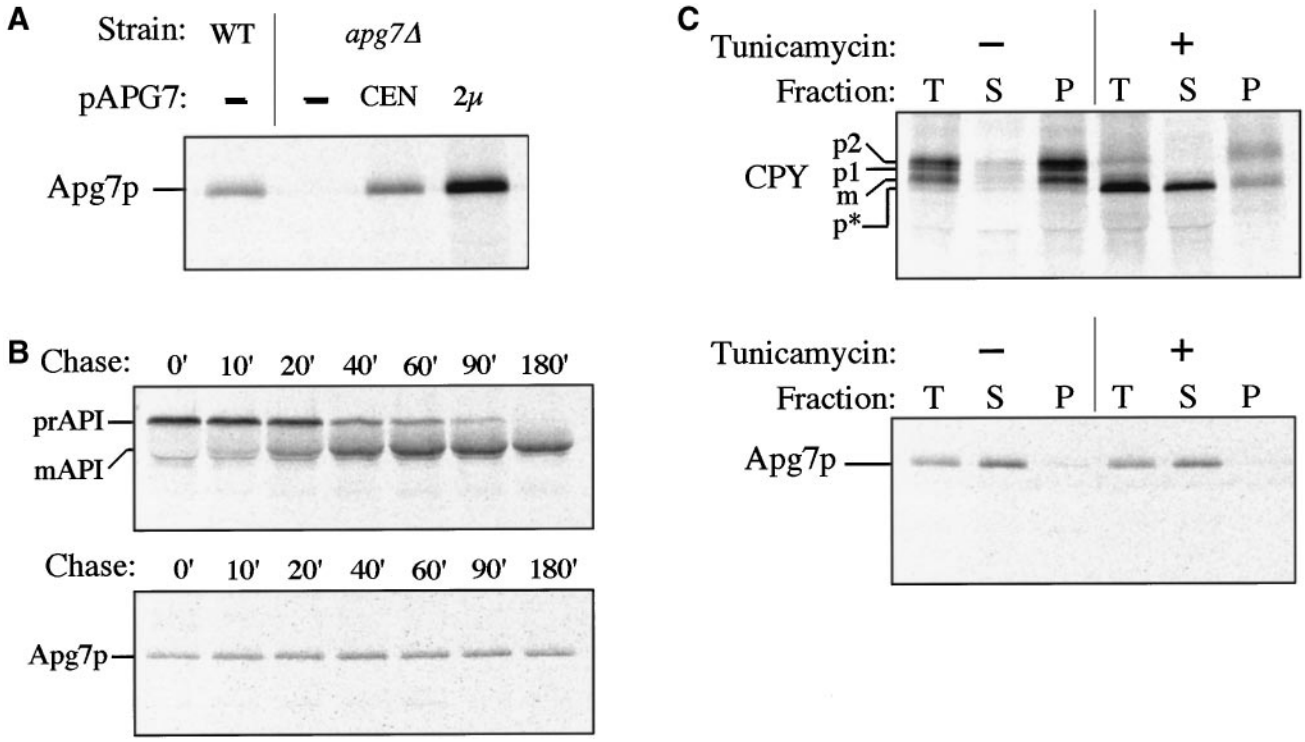

Figure 4. Apg7p is not glycosylated or proteolytically modified. (A) WT (wild-type, SEY6210), *apg7*Δ (VDY1) and the *apg7*Δ strain transformed with single-copy (CEN) or multicopy (2 μ) plasmids encoding *APG7* were grown to log phase in SMD. Cells were labeled for 10 min and immunoprecipitated with antiserum to Apg7p and analyzed by SDS-PAGE as described in MATERIALS AND METHODS. Apg7p is detected as a 71-kDa protein. (B) Wild-type (SEY6210) cells were radiolabeled for 10 min and subjected to a nonradioactive chase. At the indicated time points an aliquot was removed and precipitated with TCA. Protein extracts were prepared and successively immunoprecipitated with antiserum to API and Apg7p and analyzed as above. The positions of precursor and mature API and of Apg7p are indicated. The absence of a molecular mass shift indicates that Apg7p is not proteolytically modified. (C) Wild-type (SEY6210) cells were converted to spheroplasts and treated with tunicamycin (final concentration 20 μg/ml) to inhibit glycosylation 15 min before the addition of radioactive label as indicated. Labeling was allowed to continue for 20 min. Samples were TCA precipitated and divided in half. One-half was immunoprecipitated immediately with antiserum to CPY or Apg7p for a total (T) control. The remaining half was precipitated with Con A-Sepharose and separated into supernatant (S, not bound to Con A) and pellet (P, bound to Con A) fractions as referenced in MATERIALS AND METHODS. The separate fractions were then immunoprecipitated with antiserum to CPY or Apg7p. The positions of precursor and mature forms of glycosylated CPY (p1, p2, m) and unglycosylated precursor CPY (p*) and of Apg7p are shown. Apg7p does not bind Con A, suggesting that it is not glycosylated.

In Vivo Localization of an Apg7pGFP Fusion Protein Reveals Association with a Membrane Structure

A recent study by Ohsumi and colleagues demonstrated that Apg7p function is required for the conjugation of Apg12p to Apg5p, a reaction that is essential for macroautophagy to occur (Mizushima *et al.*, 1998). In addition, most of the Apg5p and Apg5p-Apg12p conjugate and more than half of the free Apg12p were present in 100,000 × *g* pellet fractions, suggesting that they associate with some membrane compartment. Therefore, in order for Apg7p to function in the conjugation reaction of Apg5p and Apg12p, we postulated that the site of its function would be on a membrane compartment. Alternatively, the Apg7p-mediated conjugation reaction may occur in the cytosol before membrane binding.

To investigate the subcellular location of Apg7p, we constructed a fusion of GFP to the C terminus of Apg7p and examined the localization by fluorescence microscopy. The advantage of this approach was that the localization of Apg7p could be examined in vivo. The plasmids expressing the Apg7pGFP fusion, pAPG7GFP(416) and pAPG7GFP(426), complement the API- processing defect in the *apg7*Δ strain, suggesting that the fusion proteins are functional (Figure 5A). Unfortunately, the level of fluorescence from the centromeric plasmid was below practical levels of detection. *apg7*Δ cells harboring the multicopy pAPG7GFP plasmid were grown to midlog in SMD and then shifted to SD-N medium for 15 h and visualized by

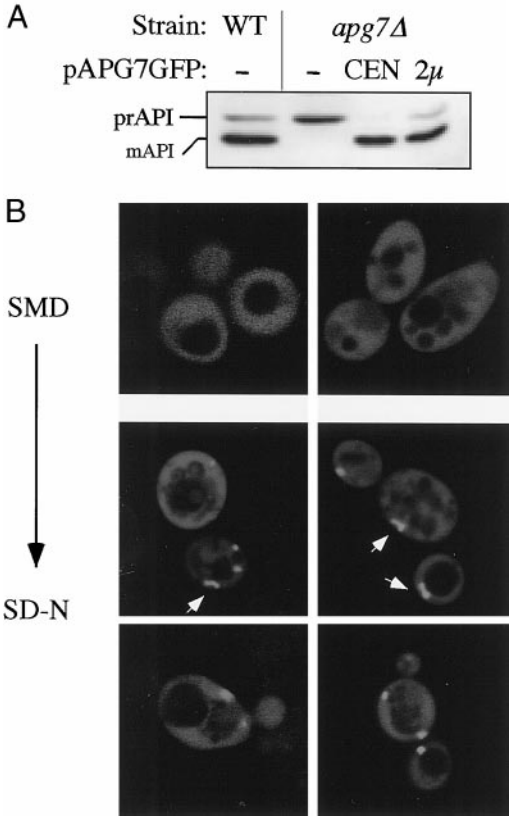

Figure 5. Apg7pGFP membrane association in vivo. (A) WT (wild-type, SEY6210), *apg7*Δ (VDY1), and the *apg7*Δ strain transformed with single-copy (CEN) or multicopy (2μ) plasmids encoding Apg7p-GFP were grown to log phase in SMD. Protein extracts were prepared and analyzed by Western blot using antiserum to API as described in MATERIALS AND METHODS. The positions of precursor and mature API are indicated. The Apg7pGFP hybrid protein complements the precursor API accumulation phenotype of the *apg7*Δ strain, indicating that the protein retains Apg7p function. (B) The *apg7*Δ strain transformed with the multicopy pAPG7GFP plasmid was grown in SMD to log phase and shifted to SD-N for 15 h. Cells from the SMD and SD-N cultures were examined by fluorescence microscopy as described in MATERIALS AND METHODS. Apg7pGFP displays primarily a diffuse cytosolic staining, but punctate structures are detected in SD-N medium. Some of the punctate structures appear rod-like in shape as indicated by arrows.

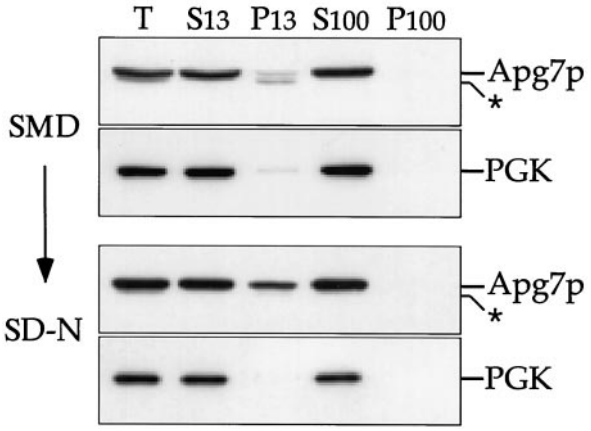

Figure 6. Apg7p subcellular fractionation pattern in SMD and SD-N. Cells from the wild-type strain (SEY6210) transformed with the multicopy plasmid encoding *APG7* were grown in SMD to midlog phase and shifted to SD-N medium for 15 h before converting them to spheroplasts. The spheroplasts were then lysed osmotically in a physiological salts buffer. After a preclearing centrifugation step at 500 × *g* for 5 min to remove unlysed spheroplasts, the total lysate (T) was separated into 13,000 × *g* supernatant (S13) and pellet (P13) fractions. The S13 fraction was further separated into 100,000 × *g* supernatant (S100) and pellet (P100) fractions. The T, S13, P13, S100, and P100 subcellular fractions were subjected to immunoblot analysis using antiserum to Apg7p and phosphoglycerate kinase (a cytosolic marker protein). A background band (*) appears below the signal for Apg7p.

confocal microscopy. Under vegetative growth conditions, the Apg7pGFP fusion protein is distributed uniformly in the cytoplasm (Figure 5B). In contrast, the Apg7pGFP fusion in cells shifted to SD-N showed both a diffuse cytoplasmic population as well as an intense punctate localization (Figure 5B). Generally found in, but not restricted to, the perivacuolar region, these punctate structures were generally circular in shape, but rod-like structures were also detected as indicated by arrows in Figure 5B. The vacuoles in cells grown in both SMD and SD-N can be seen as areas in which fluorescence is excluded. The staining pattern of Apg7p in the wild-type background appeared to be identical to the pattern in the *apg7*Δ background (our unpublished results). The shift in the Apg7pGFP localization to punctate structures under nitrogen-starvation conditions suggests that a detectable portion of Apg7p is associated with membrane structures when macroautophagy is induced.

Subcellular Fractionation of Apg7p

The analysis of Apg7pGFP suggested that we could detect a population of Apg7p associated with a membrane fraction under starvation conditions. We next performed subcellular fractionation analyses under both vegetative growth and nitrogen-starvation conditions to determine whether this observation could be confirmed biochemically. Wild-type cells transformed with the *APG7* multicopy plasmid were grown to OD_{600} = 1 in SMD medium and subsequently shifted to nitrogen-lacking SD-N medium for 15 h. Cells from both SMD and SD-N cultures were converted into spheroplasts and subjected to differential osmotic lysis as described in MATERIALS AND METHODS.

Immunoblot analysis of the subcellular fractions indicated that under vegetative growth conditions, Apg7p was predominantly localized in the S13 fraction with only a minor Apg7p band detected in the

P13 fraction (Figure 6). When the S13 sample was further separated into high-speed supernatant and pellet fractions, Apg7p remained in the soluble S100 pool. This observation is consistent with the diffuse cytosolic staining seen with the Apg7pGFP fusion protein in vegetatively growing cells (Figure 5), and the findings of Tanida *et al.* (1999), indicating that Apg7p is a cytosolic protein under vegetative conditions. In contrast, the fractionation pattern of cells shifted to SD-N for 15 h indicated that a significant portion of the Apg7p cytosolic pool now accumulated in the P13 pellet (Figure 6). Quantitation of the S13 and P13 fractions revealed that there was an increase, from 5.3% ± 0.4% to 25.2% ± 0.6%, in the amount of Apg7p found in the P13 pellet when cells were shifted from vegetative growth to nitrogen starvation conditions. The accumulation of Apg7p in the P13 fraction under SD-N conditions is consistent with the Apg7pGFP punctate localization pattern observed when cells were starved for nitrogen.

Apg7pGFP Localization to Punctate Structures Is Dependent on Apg12p

We decided to extend our analysis of Apg7p localization by examining the fluorescence pattern of the Apg7pGFP fusion protein in various mutant strains. Previous data (Mizushima *et al.*, 1998) and the studies by Yuan *et al.* (1999) and Tanida *et al.* (1999) indicate that Apg12p is conjugated to Apg7p via a thioester bond in a reaction analogous to the conjugation of ubiquitin to E1 enzymes. Furthermore, because more than half of Apg12p can be found as a membrane-associated species that pellets after a 100,000 × *g* centrifugation (Mizushima *et al.*, 1998), we hypothesized that the membrane association of Apg7pGFP may be dependent, in part, on Apg12p, its transient substrate for the conjugation reaction. To examine this possibility, Apg7pGFP was expressed in the *apg12*Δ strain and examined under vegetative and nitrogen starvation conditions. As controls, Apg7pGFP was also introduced into the wild-type and *apg5*Δ backgrounds.

The wild-type, *apg12*Δ, and *apg5*Δ strains harboring the multicopy pAPG7GFP plasmid were grown to midlog phase in SMD and then examined in SD-N over a period of 15 h (Table 1 and Figure 7). Under vegetative growth conditions, Apg7pGFP was uniformly distributed in the cytoplasm in both the *apg12*Δ and *apg5*Δ strains (our unpublished results), consistent with its localization pattern in the wild-type strain background. However, in contrast to the punctate localization of Apg7pGFP observed under nitrogen starvation conditions in the wild-type background, Apg7pGFP was unable to form these punctate structures in the *apg12*Δ strain even after shifting to SD-N. Instead, Apg7pGFP retained its uniform, cytosolic pattern (Figure 7, left panels; and Table 1), reminiscent of the Apg7pGFP distribution pattern under vegetative growth conditions. Apg7pGFP in the *apg5*Δ background maintained its punctate localization pattern in SD-N, similar to that seen in the wild-type strain. There was a qualitative difference, however, in the staining pattern of Apg7pGFP in the wild-type and *apg5*Δ backgrounds. Whereas the wild-type punctate pattern exhibited both rod-like and circular structures (Figure 5), only the latter punctate pattern could be detected in the *apg5*Δ background (Figure 7). The number of fluorescent cells exhibiting punctate structures in both the wild-type and *apg5*Δ background strains increased over time under starvation conditions while the total number of fluorescent cells remained constant over 15 h in SD-N (Table 1). These results suggest that the punctate localization of Apg7pGFP, which presumably represents its membrane associated form in vivo, is dependent on Apg12p but not Apg5p. Furthermore, a higher percentage of *apg5*Δ cells relative to wild-type displayed a punctate staining pattern after 15 h in SD-N (Table 1). This may reflect an accumulation of the Apg7p-Apg12p conjugate in the absence of Apg5p.

*GSA7, the P. pastoris Homologue to APG7, Partially Complements the API-Import Defect and the Starvation-sensitive Phenotype of apg7*Δ

In media containing methanol, the methylotrophic yeast *P. pastoris* proliferates peroxisomes and peroxisomal proteins. Upon shift of the cells to media containing glucose, excess peroxisomes are specifically degraded in the vacuole via micropexophagy (Tuttle *et al.*, 1993). The *GSA7* gene is essential to this glucose-stimulated micropexophagy pathway (Yuan *et al.*, 1999). Sequence analysis indicated that *GSA7* was the *P. pastoris* homologue of *APG7*. To determine whether Gsa7p could functionally substitute for Apg7p, we transformed *S. cerevisiae apg7*Δ cells with the *P. pastoris GSA7* gene under the control of a regulable promoter.

The *GSA7* and *APG7* genes were cloned behind the *CUP1* promoter as described in MATERIALS AND METHODS. The *apg7*Δ strain harboring either plasmid was grown in SMD lacking copper to 0.2 OD_{600}/ml and then induced for 7 h with 100 μM $CuSO_4$. Cells were then harvested and examined by immunoblot analysis. Regulation of expression was monitored by immunodetection of Apg7p (Figure 8A). The *CUP1* promoter is leaky so that a low level of Apg7p is synthesized even in the presence of the copper chelator. This amount of Apg7p is similar to the level from expression at the chromosomal locus and complements the prAPI phenotype of the *apg7*Δ strain (our unpublished results). Induction in the presence of copper results in a dramatic increase in the level of Apg7p from the pCu416APG7 plasmid (Figure 8A).

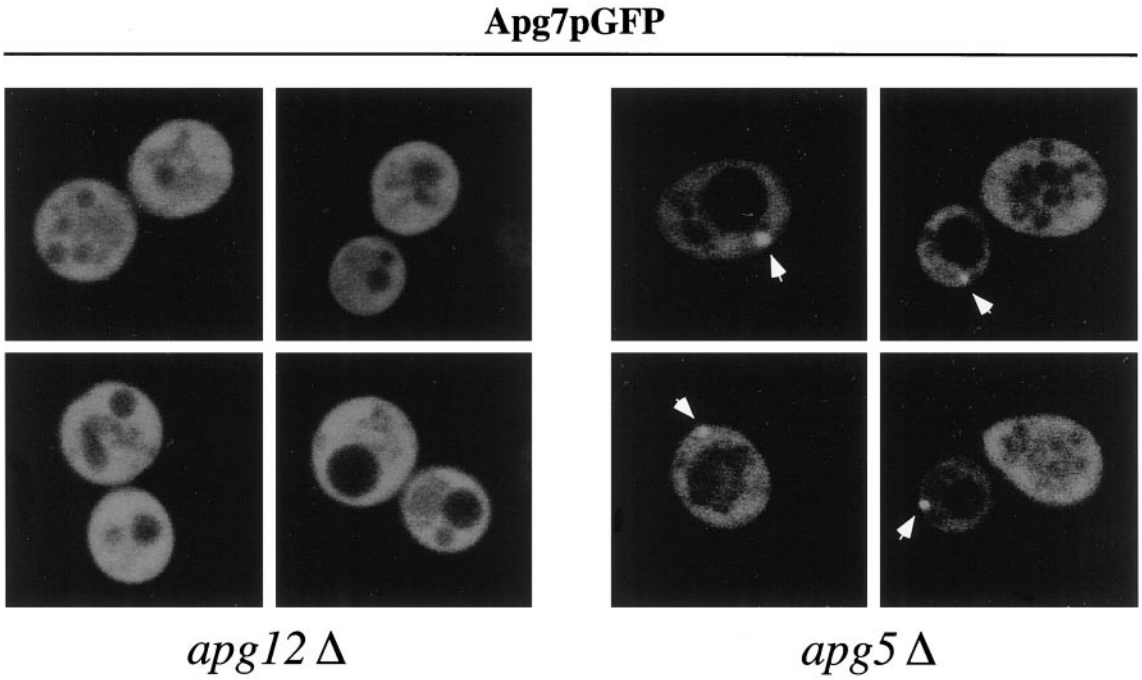

Figure 7. Membrane association of Apg7pGFP is dependent on Apg12p. The *apg5*Δ (MGY101) and *apg12*Δ (YNM101) strains transformed with the multicopy pAPG7GFP(426) plasmid were analyzed by fluorescence microscopy following transfer to SD-N as described in the legend to Figure 5. The punctate staining pattern of Apg7pGFP, marked by arrows, is dependent on the Apg12 protein.

The Gsa7 protein was not detectable with antiserum directed against Apg7p, preventing a determination of expression levels. In the absence of copper, *apg7*Δ cells harboring the pCu416GSA7 plasmid accumulated prAPI. In contrast, upon copper induction this strain showed a low but reproducible level of mature API (Figure 8B). These results indicate that at high levels, the Gsa7 protein can functionally complement the API-import defect of the *apg7*Δ strain, although only weakly. This is similar to the result seen with expression of *APG7* in the *P. pastoris gsa7* mutant (Yuan *et al.*, 1999), where the Apg7 protein is able to complement the micropexophagy defect.

Since Gsa7p partially complements the API-import defect of the *apg7*Δ strain, we further investigated whether Gsa7p would also partially rescue the nitrogen starvation defect of the *apg7*Δ strain. The *apg7*Δ strain, transformed with either pCu416GSA7 or pCu416APG7, was grown to OD_{600}=1 in SMD medium containing 100 μM $CuSO_4$ and subsequently shifted to SD-N medium. Survival under nitrogen starvation conditions was measured at the indicated times by plating aliquots onto YPD plates and counting viable colonies after 2–3 d. The results indicated that Gsa7p partially complemented the nitrogen-sensitive phenotype of the *apg7*Δ strain and demonstrates that Gsa7p can replace Apg7p in Cvt and macroautophagy pathways in *S. cerevisiae*.

DISCUSSION

In this study we have demonstrated that Apg7p is a shared component of three nonclassical pathways to the yeast vacuole in *S. cerevisiae*. The *APG7* gene complemented the API import defect of the *apg7*Δ strain under vegetative growth conditions, indicating that it is involved in the Cvt pathway (Figure 2A). In addition, *APG7* rescued the nitrogen-starvation defect in the *apg7*Δ strain, demonstrating its role in macroautophagy (Figure 2B). The *APG7* homologue, *GSA7*, in the methylotrophic yeast *P. pastoris*, is involved in the specific degradation of peroxisomes by micropexophagy (Yuan *et al.*, 1999). Expression of *GSA7* under a regulable promoter *in S. cerevisiae* partially complemented the API import defect as well as conferring greater viability during starvation conditions in the *apg7*Δ background (Figure 8). A corresponding role for Apg7p in pexophagy in *S. cerevisiae* is suggested by the finding that the *apg7*Δ strain is also defective in peroxisome degradation (Hutchins and Klionsky, manuscript in preparation). Taken together, we have demonstrated for the first time that a component of the recently characterized novel conjugation system functions in three distinct targeting pathways of Cvt, macroautophagy, and micropexophagy.

A small amount of precursor API was reproducibly detected when *APG7* was expressed on a multicopy

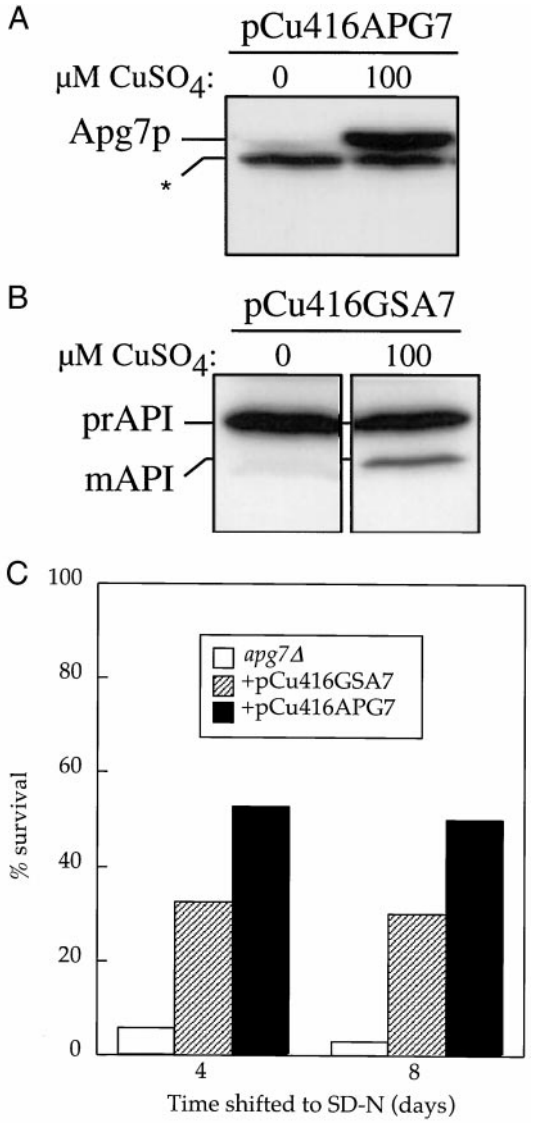

Figure 8. The *Pichia pastoris* GSA7 gene partially complements the *apg7* defect. (A) The *apg7*Δ strain (VDY1) was transformed with a plasmid encoding the *APG7* gene cloned behind the regulable *CUP1* promoter (pCu416APG7). Cells were grown in YNB minus copper containing either 100 μM BCS copper chelator or 100 μM copper sulfate. After 7 h, cells were TCA precipitated, and the protein extract was analyzed by immunoblot using antiserum to Apg7p. Induction by copper results in a significant increase in Apg7p synthesis. A background band has been indicated by an asterisk (*). (B) The *apg7*Δ strain was transformed with a plasmid encoding the *GSA7* gene cloned behind the regulable *CUP1* promoter (pCu416GSA7). Cells were grown as above and analyzed by immunoblot with antiserum to API. The *GSA7* gene partially complements the *apg7* defect. (C) The *apg7*Δ strain transformed with the pCu416GSA7 or the pCu416APG7 plasmid was grown in YNB minus copper containing 100 μM coppper sulfate and transferred to SD-N as described in MATERIALS AND METHODS. Aliquots were removed at the indicated times and spread onto YPD plates in triplicate. Numbers of viable colonies were determined after 2–3 d. The pCu416GSA7 plasmid partially complements the starvation-sensitive phenotype of the *apg7*Δ mutant.

plasmid (Figure 2A). The precursor API accumulation phenotype increased when *APG7* was expressed at higher levels under the control of the regulable *CUP1* promoter on a multicopy plasmid (our unpublished results). These findings suggest that overexpression of Apg7p may have a saturating effect on other components in the API-import pathway.

The site of accumulated precursor API in the *apg7*Δ strain was found to be part of a membrane-associated, large protein complex, presumably the Cvt complex, that was pelletable upon detergent treatment (Figure 3A). In addition, prAPI was accessible to exogenously added protease, suggesting that the vesicle around the Cvt complex had not formed completely. These experiments place the action of Apg7p at a step of vesicle formation around the Cvt complex in vegetative conditions or around cytosol during starvation (Figure 1, step 4). Experiments on the biogenesis of Apg7p indicated that this 71-kDa protein was not posttranslationally modified by proteolytic processing or glycosylation (Figure 4). Tanida *et al.* (1999) demonstrate that Apg12p is conjugated to Apg7p via a thioester modification and that the two proteins can be coimmunoprecipitated. Due to the reducing conditions of our pulse/chase labeling conditions, we did not detect this event.

The subcellular localization of Apg7p was determined biochemically by subcellular fractionations and in vivo through the use of a fusion of Apg7p with GFP. The biochemical fractionations localized Apg7p predominantly to a soluble S100 fraction under vegetative growth conditions, suggesting a cytosolic localization. The shift to starvation conditions resulted in a small but significant amount of Apg7p to be localized to a low-speed P13 pellet (Figure 6). The association of Apg7p with the P13 pellet fractionation was sensitive to extended lysis times; reproducible results were obtained only when the lysis and subsequent centrifugation steps were performed immediately after lysis. We believe this is indicative of a weak interaction of Apg7p with the P13 pellet fraction. The in vivo examination of the Apg7pGFP fusion protein indicated that a portion of the Apg7pGFP was localized to strongly staining punctate structures that could be detected under nitrogen starvation conditions (Figure 5). This punctate localization of Apg7pGFP was dependent on the presence of Apg12p but not Apg5p (Figure 7). Apg12p shows a partially pelletable distribution in the cell (Mizushima *et al.*, 1998). One interpretation of the fluorescence data is that the punctate pattern for Apg7p represents the intermediate Apg7p-Apg12p conjugate. The formation of punctate Apg7pGFP structures under starvation conditions is consistent with the accumulation of a small amount of Apg7p to the P13 pellet fraction in our biochemical fractionation experiments.

The conjugation of Apg12p to Apg7p has been demonstrated to be required for both API import and autophagy by Tanida *et al.* (1999). Therefore, if the site of action of Apg7p is on the membrane of the punctate structures seen under nitrogen starvation conditions, why aren't these structures also seen under vegetative growth conditions? This may be due to the limitations of fluorescence microscopy in detecting the significantly smaller size of the vesicles being formed during vegetative growth (Cvt vesicles, 150 nm diameter) versus those that are formed under starvation conditions (autophagosomes, 300–900 nm diameter). In addition, electron microscopy data suggest that the number of Cvt vesicles formed during vegetative growth is substantially lower than the number of autophagosomes that are generated during starvation. Because association of Apg7p with Apg12p is transient, there is a greater likelihood of detecting this interaction in starvation conditions.

The requirement for Apg7p-dependent conjugation in both rich and starvation conditions suggests that conjugation is not a regulatory step. The reactions that occur during conjugation, however, may be regulated by other factors. For example, in micropexophagy, invaginations of the vacuolar membrane or finger-like protrusions from the vacuole are thought to capture the targeted peroxisomes and sequester them inside the vacuole for degradation. In the study by Yuan *et al.* (1999), electron micrographs show that the micropexophagy defect in the *gsa7* strain appears to be in the completion of vacuole membrane fusion around peroxisomes. Accordingly, the site of action of the Gsa7p in *P. pastoris* appears to be at the vacuolar membrane. In addition, Yuan *et al.* (1999), indicate that the *gsa7* mutant is defective in protein turnover under starvation conditions, suggesting that Gsa7p is also required for macroautophagy in the yeast *P. pastoris*. Similarly, the proposed site of Apg7p function in *S. cerevisiae* is at the formation or completion of the autophagosome or Cvt vesicle. This dual function in micropexophagy and macroautophagy may reflect the role of accessory proteins that differentially target Apg7p/Gsa7p and, by extension, the conjugation system, depending on the nutrient conditions. Alternatively, the vacuole membrane may serve as the donor membrane compartment for the formation of the autophagosome and Cvt vesicle via retrograde movement from this organelle. In this case, the *apg7* and *gsa7* mutants would both be blocked in events involving sequestration by vacuolar membrane.

We have demonstrated that Apg7p functions in three nonclassical targeting pathways to the yeast vacuole. The fact that *APG7* homologues exist in higher eukaryotes including humans indicates the function of this novel conjugation system, which includes Apg7p, Apg12p, and Apg5p, may be as a conserved, general targeting mechanism for a variety of nonclassical pathways to the vacuole/lysosome.

ACKNOWLEDGMENTS

We thank Dr. Heiner Matthies and Dawn Signor for assistance with confocal microscopy. This work was supported by a National Institutes of Health Molecular and Cellular Biology training grant to J.K. and K.P.E., a National Science Foundation Plant Cell Biology training grant to V.M.D., an American Cancer Society, California Division Senior Postdoctoral Fellowship to S.V.S., and by Public Health Service grant GM-53396 from the National Institutes of Health to D.J.K.

REFERENCES

Baba, M., Osumi, M., and Ohsumi, Y. (1995). Analysis of the membrane structures involved in autophagy in yeast by freeze-replica method. Cell Struct. Funct. *20*, 465–471.

Baba, M., Osumi, M., Scott, S.V., Klionsky, D.J., and Ohsumi, Y. (1997). Two distinct pathways for targeting proteins from the cytoplasm to the vacuole/lysosome. J. Cell Biol. *139*, 1687–1695.

Baba, M., Takeshige, K., Baba, N., and Ohsumi, Y. (1994). Ultrastructural analysis of the autophagic process in yeast: detection of autophagosomes and their characterization. J. Cell Biol. *124*, 903–913.

Babst, M., Sato, T.K., Banta, L.M., and Emr, S.D. (1997). Endosomal transport function in yeast requires a novel AAA-type ATPase, Vps4p. EMBO J. *16*, 1820–1831.

Baum, P., Thorner, J., and Honig, L. (1978). Identification of tubulin from the yeast *Saccharomyces cerevisiae*. Proc. Natl. Acad. Sci. USA *75*, 4962–4966.

Bryant, N.J., and Stevens, T.H. (1998). Vacuole biogenesis in *Saccharomyces cerevisiae*: protein transport pathways to the yeast vacuole. Microbiol. Mol. Biol. Rev. *62*, 230–247.

Darsow, T., Rieder, S.E., and Emr, S.D. (1997). A multispecificity syntaxin homologue, Vam3p, esential for autophagic and biosynthetic protein transport to the vacuole. J. Cell Biol. *138*, 517–529.

Funakoshi, T., Matsuura, A., Noda, T., and Ohsumi, Y. (1997). Analyses of *APG13* gene involved in autophagy in yeast. *Saccharomyces cerevisiae*. Gene *192*, 207–213.

Haas, A., Scheglmann, D., Lazar, T., Gallwitz, D., and Wickner, W. (1995). The GTPase Ypt7p of *Saccharomyces cerevisiae* is required on both partner vacuoles for the homotypic fusion step of vacuole inheritance. EMBO J. *14*, 5258–5270.

Harding, T.M., Hefner-Gravink, A., Thumm, M., and Klionsky, D.J. (1996). Genetic and phenotypic overlap between autophagy and the cytoplasm to vacuole protein targeting pathway. J. Biol. Chem. *271*, 17621–17624.

Harding, T.M., Morano, K.A., Scott, S.V., and Klionsky, D.J. (1995). Isolation and characterization of yeast mutants in the cytoplasm to vacuole protein targeting pathway. J. Cell Biol. *131*, 591–602.

Kametaka, S., Matsuura, A., Wada, Y., and Ohsumi, Y. (1996). Structural and functional analyses of *APG5*, a gene involved in autophagy in yeast. Gene *178*, 139–143.

Kiel, J.A.K.W., Rechinger, K.B., van der Klei, I.J., Salomons, F.A., Titorenko, V.I., and Veenhuis, M. (1999). The *Hansenula polymorpha PDD1* gene, essential for selective degradation of peroxisomes, is a homologue of *Saccharomyces cerevisiae* Vps34. Yeast (*in press*).

Kim, J., Scott, S.V., Oda, M., and Klionsky, D.J. (1997). Transport of a large oligomeric protein by the cytoplasm to vacuole protein targeting pathway. J. Cell Biol., *137*, 609–618.

Klionsky, D.J. (1997). Protein transport from the cytoplasm into the vacuole. J. Membr. Biol. *157*, 105–115.

Klionsky, D.J. (1998). Nonclassical protein sorting to the yeast vacuole. J. Biol. Chem. *273*, 10807–10810.

Klionsky, D.J., Banta, L.M., and Emr, S.D. (1988). Intracellular sorting and processing of a yeast vacuolar hydrolase: proteinase A propeptide contains vacuolar targeting information. Mol. Cell. Biol. *8*, 2105–2116.

Klionsky, D.J., Cueva, R., and Yaver, D.S. (1992). Aminopeptidase I of *Saccharomyces cerevisiae* is localized to the vacuole independent of the secretory pathway. J. Cell Biol. *119*, 287–299.

Klionsky, D.J., Herman, P.K., and Emr, S.D. (1990). The fungal vacuole: composition, function, and biogenesis. Microbiol. Rev. *54*, 266–292.

Labbe, S., and Thiele, D.J. (1999). Copper ion inducible and repressible promoter systems in yeast. Methods Enzymol. (*in press*).

Lang, T., Schaeffeler, E., Bernreuther, D., Bredschneider, M., Wolf, D.H., and Thumm, M. (1998). Aut2p and Aut7p, two novel microtubule-associated proteins are essential for delivery of autophagic vesicles to the vacuole. EMBO J. *17*, 3597–3607.

Matsuura, A., Tsukada, M., Wada, Y., and Ohsumi, Y. (1997). Apg1p, a novel protein kinase required for the autophagic process in *Saccharomyces cerevisiae*. Gene *192*, 245–50.

Mizushima, N., Noda, T., Yoshimori, T., Tanaka, Y., Ishii, T., George, M.D., Klionsky, D.J., Ohsumi, M., and Ohsumi, Y. (1998). A protein conjugation sytem essential for autophagy. Nature *395*, 395–398.

Nakamura, N., Matsuura, A., Wada, Y., and Ohsumi, Y. (1997). Acidification of vacuole is required for the autophagic degradation in the yeast *Saccharomyces cerevisiae*. J. Biochem. *121*, 338–344.

Oda, M.N., Scott, S.V., Hefner-Gravink, A., Caffarelli, A.D., and Klionsky, D.J. (1996). Identification of a cytoplasm to vacuole targeting determinant in aminopeptidase I. J. Cell Biol. *132*, 999–1010.

Riezman, H., Munn, A., Geli, M.I., and Hicke, L. (1996). Actin-, myosin- and ubiquitin-dependent endocytosis. Experientia *52*, 1033–1041.

Robinson, J.S., Klionsky, D.J., Banta, L.M., and Emr, S.D. (1988). Protein sorting in *Saccharomyces cerevisiae*: isolation of mutants defective in the delivery and processing of multiple vacuolar hydrolases. Mol. Cell. Biol. *8*, 4936–4948.

Rose, M.D., Novick, P., Thomas, J.H., Botstein, D., and Fink, G.R. (1987). A *Saccharomyces cerevisiae* genomic plasmid bank based on a centromere-containing shuttle vector. Gene *60*, 237–243.

Sakai, Y., Koller, A., Rangell, L.K., Keller, G.A., and Subramani, S. (1998). Peroxisome degradation by microautophagy in *Pichia pastoris*: identification of specific steps and morphological intermediates. J. Cell Biol. *141*, 625–636.

Schlumpberger, M., Schaeffeler, E., Straub, M., Bredschneider, M., Wolf, D.H., and Thumm, M. (1997). *AUT1*, a gene essential for autophagocytosis in the yeast *Saccharomyces cerevisiae*. J. Bacteriol. *179*, 1068–1076.

Scott, S.V., Baba, M., Ohsumi, Y., and Klionsky, D.J. (1997). Aminopeptidase I is targeted to the vacuole by a nonclassical vesicular mechanism. J. Cell Biol. *138*, 37–44.

Scott, S.V., Hefner-Gravink, A., Morano, K.A., Noda, T., Ohsumi, Y., and Klionsky, D.J. (1996). Cytoplasm-to-vacuole targeting and autophagy employ the same machinery to deliver proteins to the yeast vacuole. Proc. Natl. Acad. Sci. USA *93*, 12304–12308.

Scott, S.V., and Klionsky, D.J. (1998). Delivery of proteins and organelles to the vacuole from the cytoplasm. Curr. Opin. Cell Biol. *10*, 523–529.

Straub, M., Bredschneider, M., and Thumm, M. (1997). *AUT3*, a serine/threonine kinase gene, is essential for autophagocytosis in *Saccharomyces cerevisiae*. J. Bacteriol. *179*, 3875–3883.

Takeshige, K., Baba, M., Tsuboi, S., Noda, T., and Ohsumi, Y. (1992). Autophagy in yeast demonstrated with proteinase-deficient mutants and conditions for its induction. J. Cell Biol. *119*, 301–311.

Tanida, I., Mizushima, N., Kiyooka, M., Ohsumi, M., Ueno, T., Ohsumi, Y., and Kominami, E. (1999). Apg7p/Cvt2p: a novel protein activating enzyme essential for autophagy. Mol. Biol. Cell *10*, 1367–1379.

Thumm, M., Egner, R., Koch, M., Schlumpberger, M., Straub, M., Veenhuis, M., and Wolf, D.H. (1994). Isolation of autophagocytosis mutants of *Saccharoymces cerevisiae*. FEBS Lett. *349*, 275–280.

Titorenko, V.I., Keizer, I., Harder, W., and Veenhuis, M. (1995). Isolation and characterization of mutants impaired in the selective degradation of peroxisomes in the yeast *Hansenula polymorpha*. J. Bacteriol. *177*, 357–363.

Tsukada, M., and Ohsumi, Y. (1993). Isolation and characterization of autophagy-defective mutants of *Saccharomyces cerevisiae*. FEBS Lett. *333*, 169–174.

Tuttle, D.L., and Dunn, W.A., Jr. (1995). Divergent modes of autophagy in the methylotrophic yeast *Pichia pastoris*. J. Cell Sci. *108*, 25–35.

Tuttle, D.L., Lewin, A.S., and Dunn, W.A., Jr. (1993). Selective autophagy of peroxisomes in methylotrophic yeasts. Eur. J. Cell Biol. *60*, 283–290.

Wurmser, A.E., and Emr, S.D. (1998). Phosphoinositide signaling and turnover: PtdIns(3)P, a regulator of membrane traffic, is transported to the vacuole and degraded by a process that requires lumenal vacuolar hydrolase activities. EMBO J. *17*, 4930–4942.

Yuan, W., Strombaug, P.E., and Dunn, W.A., Jr. (1999). Glucose-induced autophagy of peroxisomes in *Pichia pastoris* requires a unique E1-like protein. Mol. Biol. Cell *10*, 1353–1366.

Yuan, W.Y., Tuttle, D.L., Shi, Y.-J., Ralph, G.S., and Dunn, W.A., Jr. (1997). Glucose-induced microautophagy in *Pichia pastoris* requires the α-subunit of phosphofructokinase. J. Cell Sci. *110*, 1935–1945.